
Exact expressions for double descent and implicit regularization via surrogate random design

Anonymous Author(s)

Affiliation

Address

email

Abstract

Double descent refers to the phase transition that is exhibited by the generalization error of unregularized learning models when varying the ratio between the number of parameters and the number of training samples. The recent success of highly over-parameterized machine learning models such as deep neural networks has motivated a theoretical analysis of the double descent phenomenon in classical models such as linear regression which can also generalize well in the over-parameterized regime. We provide the first exact non-asymptotic expressions for double descent of the minimum norm linear estimator. Our approach involves constructing a special determinantal point process which we call surrogate random design, to replace the standard i.i.d. design of the training sample. This surrogate design admits exact expressions for the mean squared error of the estimator while preserving the key properties of the standard design. We also establish an exact implicit regularization result for over-parameterized training samples. In particular, we show that, for the surrogate design, the implicit bias of the unregularized minimum norm estimator precisely corresponds to solving a ridge-regularized least squares problem on the population distribution. In our analysis we introduce a new mathematical tool of independent interest: the class of random matrices for which determinant commutes with expectation.

1 Introduction

Classical statistical learning theory asserts that to achieve generalization one must use training sample size that sufficiently exceeds the complexity of the learning model, where the latter is typically represented by the number of parameters [or some related structural parameter; see FHT01]. In particular, this seems to suggest the conventional wisdom that one should not use models that fit the training data exactly. However, modern machine learning practice often seems to go against this intuition, using models with so many parameters that the training data can be perfectly interpolated, in which case the training error vanishes. It has been shown that models such as deep neural networks, as well as certain so-called interpolating kernels and decision trees, can generalize well in this regime. In particular, [BHMM19] empirically demonstrated a phase transition in generalization performance of learning models which occurs at an *interpolation threshold*, i.e., a point where training error goes to zero (as one varies the ratio between the model complexity and the sample size). Moving away from this threshold in either direction tends to reduce the generalization error, leading to the so-called *double descent* curve.

To understand this surprising phenomenon, in perhaps the simplest possible setting, we study it in the context of linear or least squares regression. Consider a full rank $n \times d$ data matrix \mathbf{X} and a vector \mathbf{y} of responses corresponding to each of the n data points (the rows of \mathbf{X}), where we wish to find the best linear model $\mathbf{X}\mathbf{w} \approx \mathbf{y}$, parameterized by a d -dimensional vector \mathbf{w} . The simplest

example of an estimator that has been shown to exhibit the double descent phenomenon [BHX19] is the Moore-Penrose estimator, $\hat{\mathbf{w}} = \mathbf{X}^\dagger \mathbf{y}$: in the so-called over-determined regime, i.e., when $n > d$, it corresponds to the least squares solution, i.e., $\operatorname{argmin}_{\mathbf{w}} \|\mathbf{X}\mathbf{w} - \mathbf{y}\|^2$; and in the under-determined regime (also known as over-parameterized or interpolating), i.e., when $n < d$, it corresponds to the minimum norm solution to the linear system $\mathbf{X}\mathbf{w} = \mathbf{y}$. Given the ubiquity of linear regression and the Moore-Penrose solution, e.g., in kernel-based machine learning, studying the performance of this estimator can shed some light on the effects of over-parameterization/interpolation in machine learning more generally. Of particular interest are results that are exact (i.e., not upper/lower bounds) and non-asymptotic (i.e., for large but still finite n and d).

We build on methods from Randomized Numerical Linear Algebra (RandNLA) in order to obtain *exact non-asymptotic expressions* for the mean squared error (MSE) of the Moore-Penrose estimator (see Theorem 1). This provides a precise characterization of the double descent phenomenon for the linear regression problem. In obtaining these results, we are able to provide precise formulas for the *implicit regularization* induced by minimum norm solutions of under-determined training samples, relating it to classical ridge regularization (see Theorem 2). To obtain our precise results, we use a somewhat non-standard random design, based on a specially chosen determinantal point process (DPP), which we term surrogate random design. DPPs are a family of non-i.i.d. sampling distributions which are typically used to induce diversity in the produced samples [KT12]. Our aim in using a DPP as a surrogate design is very different: namely, to make certain quantities (such as the MSE) analytically tractable, while accurately *preserving* the underlying properties of the original data distribution. This strategy might seem counter-intuitive since DPPs are typically found most useful when they *differ* from the data distribution. However, we show both theoretically (Theorem 3) and empirically (Section 5), that for many commonly studied data distributions, such as multivariate Gaussians, our DPP-based surrogate design accurately preserves the key properties of the standard i.i.d. design (such as the MSE), and even matches it exactly in the high-dimensional asymptotic limit. In our analysis of the surrogate design, we introduce the concept of *determinant preserving random matrices* (Section 4), a class of random matrices for which determinant commutes with expectation, which should be of independent interest.

1.1 Main results: double descent and implicit regularization

As the performance metric in our analysis, we use the *mean squared error* (MSE), defined as $\operatorname{MSE}[\hat{\mathbf{w}}] = \mathbb{E}[\|\hat{\mathbf{w}} - \mathbf{w}^*\|^2]$, where \mathbf{w}^* is a fixed underlying linear model of the responses. In analyzing the MSE, we make the following standard assumption that the response noise is homoscedastic.

Assumption 1 (Homoscedastic noise) *The noise $\xi = y(\mathbf{x}) - \mathbf{x}^\top \mathbf{w}^*$ has mean 0 and variance σ^2 .*

Our main result provides an exact expression for the MSE of the Moore-Penrose estimator under our surrogate design denoted $\bar{\mathbf{X}} \sim S_\mu^n$, where μ is the d -variate distribution of the row vector \mathbf{x}^\top and n is the sample size. This surrogate is used in place of the standard $n \times d$ random design $\mathbf{X} \sim \mu^n$, where n data points (the rows of \mathbf{X}) are sampled independently from μ . We form the surrogate by constructing a determinantal point process with μ as the background measure, so that $S_\mu^n(\mathbf{X}) \propto \operatorname{pdet}(\mathbf{X}\mathbf{X}^\top)\mu(\mathbf{X})$, where $\operatorname{pdet}(\cdot)$ denotes the pseudo-determinant (details in Section 3). Unlike for the standard design, our MSE formula is fully expressible as a function of the covariance matrix $\Sigma_\mu = \mathbb{E}_\mu[\mathbf{x}\mathbf{x}^\top]$. To state our main result, we need an additional minor assumption on μ which is satisfied by most standard continuous distributions (e.g., multivariate Gaussians).

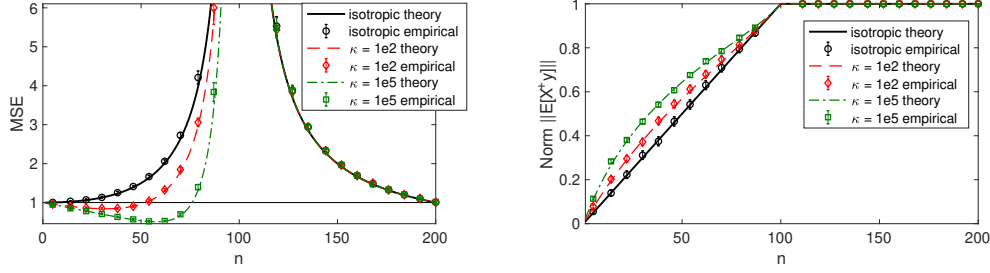
Assumption 2 (General position) *For $1 \leq n \leq d$, if $\mathbf{X} \sim \mu^n$, then $\operatorname{rank}(\mathbf{X}) = n$ almost surely.*

Under Assumptions 1 and 2, we can establish our first main result, stated as the following theorem, where we use \mathbf{X}^\dagger to denote the Moore-Penrose inverse of \mathbf{X} .

Theorem 1 (Exact non-asymptotic MSE) *If the response noise is homoscedastic (Assumption 1) and μ is in general position (Assumption 2), then for $\bar{\mathbf{X}} \sim S_\mu^n$ (Definition 3) and $\bar{y}_i = y(\bar{\mathbf{x}}_i)$,*

$$\operatorname{MSE}[\bar{\mathbf{X}}^\dagger \bar{\mathbf{y}}] = \begin{cases} \sigma^2 \operatorname{tr}((\Sigma_\mu + \lambda_n \mathbf{I})^{-1}) \cdot \frac{1-\alpha_n}{d-n} + \frac{\mathbf{w}^{*\top}(\Sigma_\mu + \lambda_n \mathbf{I})^{-1} \mathbf{w}^*}{\operatorname{tr}(\Sigma_\mu + \lambda_n \mathbf{I})^{-1}} \cdot (d-n), & \text{for } n < d, \\ \sigma^2 \operatorname{tr}(\Sigma_\mu^{-1}), & \text{for } n = d, \\ \sigma^2 \operatorname{tr}(\Sigma_\mu^{-1}) \cdot \frac{1-\beta_n}{n-d}, & \text{for } n > d, \end{cases}$$

with $\lambda_n \geq 0$ defined by $n = \operatorname{tr}(\Sigma_\mu(\Sigma_\mu + \lambda_n \mathbf{I})^{-1})$, $\alpha_n = \det(\Sigma_\mu(\Sigma_\mu + \lambda_n \mathbf{I})^{-1})$ and $\beta_n = e^{d-n}$.



(a) Surrogate MSE expressions (Theorem 1) closely match numerical estimates even for non-isotropic features. Eigenvalue decay leads to a steeper descent curve in the under-determined regime ($n < d$).

(b) The mean of the estimator $\mathbf{X}^\dagger \mathbf{y}$ exhibits shrinkage which closely matches the shrinkage of a ridge-regularized least squares optimum (theory lines), as characterized by Theorem 2.

Figure 1: Illustration of the main results for $d = 100$ and $\mu = \mathcal{N}(\mathbf{0}, \Sigma)$ where Σ is diagonal with eigenvalues decaying exponentially and scaled so that $\text{tr}(\Sigma^{-1}) = d$. We use our surrogate formulas to plot (a) the MSE (Theorem 1) and (b) the norm of the expectation (Theorem 2) of the Moore-Penrose estimator (theory lines), accompanied by the empirical estimates based on the standard i.i.d. design (error bars are three times the standard error of the mean). We consider three different condition numbers κ of Σ , with *isotropic* corresponding to $\kappa = 1$, i.e., $\Sigma = \mathbf{I}$. We use $\sigma^2 = 1$ and $\mathbf{w}^* = \frac{1}{\sqrt{d}} \mathbf{1}$.

85 **Definition 1** We will use $\mathcal{M} = \mathcal{M}(\Sigma_\mu, \mathbf{w}^*, \sigma^2, n)$ to denote the above expressions for $\text{MSE}[\bar{\mathbf{X}}^\dagger \bar{\mathbf{y}}]$.

86 Proof of Theorem 1 is given in Appendix C. For illustration, we plot the MSE expressions in Figure 1a,
 87 comparing them with empirical estimates of the true MSE under the i.i.d. design for a multivariate
 88 Gaussian distribution $\mu = \mathcal{N}(\mathbf{0}, \Sigma)$ with several different covariance matrices Σ . We keep the
 89 number of features d fixed to 100 and vary the number of samples n , observing a double descent peak
 90 at $n = d$. We observe that our theory aligns well with the empirical estimates, whereas previously, no
 91 such theory was available except for special cases such as $\Sigma = \mathbf{I}$ (more details in Theorem 3 and
 92 Section 5). The plots show that varying the spectral decay of Σ has a significant effect on the shape
 93 of the curve in the under-determined regime. We use the horizontal line to denote the MSE of the null
 94 estimator $\text{MSE}[\mathbf{0}] = \|\mathbf{w}^*\|^2 = 1$. When the eigenvalues of Σ decay rapidly, then the Moore-Penrose
 95 estimator suffers less error than the null estimator for some values of $n < d$, and the curve exhibits a
 96 local optimum in this regime.

97 One important aspect of Theorem 1 comes from the relationship between n and the parameter λ_n ,
 98 which together satisfy $n = \text{tr}(\Sigma_\mu(\Sigma_\mu + \lambda_n \mathbf{I})^{-1})$. This expression is precisely the classical notion of
 99 *effective dimension* for ridge regression regularized with λ_n [AM15], and it arises here even though
 100 there is no explicit ridge regularization in the problem being considered in Theorem 1. The global
 101 solution to the ridge regression task (i.e., ℓ_2 -regularized least squares) with parameter λ is defined as:

$$\underset{\mathbf{w}}{\text{argmin}} \left\{ \mathbb{E}_{\mu, y} [(\mathbf{x}^\top \mathbf{w} - y(\mathbf{x}))^2] + \lambda \|\mathbf{w}\|^2 \right\} = (\Sigma_\mu + \lambda \mathbf{I})^{-1} \mathbf{v}_{\mu, y}, \quad \text{where } \mathbf{v}_{\mu, y} = \mathbb{E}_{\mu, y} [y(\mathbf{x}) \mathbf{x}].$$

102 When Assumption 1 holds, then $\mathbf{v}_{\mu, y} = \Sigma_\mu \mathbf{w}^*$, however ridge-regularized least squares is well-
 103 defined for much more general response models. Our second result makes a direct connection
 104 between the (expectation of the) unregularized minimum norm solution on the sample and the global
 105 ridge-regularized solution. While the under-determined regime (i.e., $n < d$) is of primary interest
 106 to us, for completeness we state this result for arbitrary values of n and d . Note that, just like the
 107 definition of regularized least squares, this theorem applies more generally than Theorem 1, in that it
 108 does *not* require the responses to follow any linear model as in Assumption 1 (proof in Appendix D).

109 **Theorem 2 (Implicit regularization of Moore-Penrose estimator)** For μ satisfying Assumption 2
 110 and $y(\cdot)$ s.t. $\mathbf{v}_{\mu, y} = \mathbb{E}_{\mu, y} [y(\mathbf{x}) \mathbf{x}]$ is well-defined, $\bar{\mathbf{X}} \sim S_\mu^n$ (Definition 3) and $\bar{y}_i = y(\bar{\mathbf{x}}_i)$,

$$\mathbb{E}[\bar{\mathbf{X}}^\dagger \bar{\mathbf{y}}] = \begin{cases} (\Sigma_\mu + \lambda_n \mathbf{I})^{-1} \mathbf{v}_{\mu, y} & \text{for } n < d, \\ \Sigma_\mu^{-1} \mathbf{v}_{\mu, y} & \text{for } n \geq d, \end{cases}$$

111 where, as in Theorem 1, λ_n is such that the effective dimension $\text{tr}(\Sigma_\mu(\Sigma_\mu + \lambda_n \mathbf{I})^{-1})$ equals n .

That is, when $n < d$, the Moore-Penrose estimator (which itself is not regularized), computed on the random training sample, in expectation equals the global ridge-regularized least squares solution of the underlying regression problem. Moreover, λ_n , i.e., the amount of implicit ℓ_2 -regularization, is controlled by the degree of over-parameterization in such a way as to ensure that n becomes the ridge effective dimension (a.k.a. the effective degrees of freedom).

We illustrate this result in Figure 1b, plotting the norm of the expectation of the Moore-Penrose estimator. As for the MSE, our surrogate theory aligns well with the empirical estimates for i.i.d. Gaussian designs, showing that the shrinkage of the unregularized estimator in the under-determined regime matches the implicit ridge-regularization characterized by Theorem 2. While the shrinkage is a linear function of the sample size n for isotropic features (i.e., $\Sigma = \mathbf{I}$), it exhibits a non-linear behavior for other spectral decays. Such *implicit regularization* has been studied previously [see, e.g., MO11, Mah12]; it has been observed empirically for RandNLA sampling algorithms [MMY15]; and it has also received attention more generally within the context of neural networks [Ney17]. While our implicit regularization result is limited to the Moore-Penrose estimator, this new connection (and others, described below) between the minimum norm solution of an unregularized under-determined system and a ridge-regularized least squares solution offers a simple interpretation for the implicit regularization observed in modern machine learning architectures.

Our exact non-asymptotic expressions in Theorem 1 and our exact implicit regularization results in Theorem 2 are derived for the surrogate design, which is a non-i.i.d. distribution based on a determinantal point process. However, Figure 1 suggests that those expressions accurately describe the MSE (up to lower order terms) also under the standard i.i.d. design $\mathbf{X} \sim \mu^n$ when μ is a multivariate Gaussian. As a third result, we verify that the surrogate expressions for the MSE are asymptotically consistent with the MSE of an i.i.d. design, for a wide class of distributions which include multivariate Gaussians.

Theorem 3 (Asymptotic consistency of surrogate design) *Let $\mathbf{X} \in \mathbb{R}^{n \times d}$ have i.i.d. rows $\mathbf{x}_i^\top = \mathbf{z}_i^\top \Sigma^{\frac{1}{2}}$ where \mathbf{z}_i has independent zero mean and unit variance sub-Gaussian entries, and suppose that Assumptions 1 and 2 are satisfied. Furthermore, suppose that there exist $c, C, C^* \in \mathbb{R}_{>0}$ such that $C\mathbf{I} \succeq \Sigma \succeq c\mathbf{I} \succ 0$ and $\|\mathbf{w}^*\| \leq C^*$. Then*

$$\text{MSE}[\mathbf{X}^\dagger \mathbf{y}] - \mathcal{M}(\Sigma, \mathbf{w}^*, \sigma^2, n) \rightarrow 0$$

with probability one as $d, n \rightarrow \infty$ with $n/d \rightarrow \bar{c} \in (0, \infty) \setminus \{1\}$.

The above result is particularly remarkable since our surrogate design is a determinantal point process. DPPs are commonly used in ML to ensure that the data points in a sample are well spread-out. However, if the data distribution is sufficiently regular (e.g., a multivariate Gaussian), then the i.i.d. samples are already spread-out reasonably well, so rescaling the distribution by a determinant has a negligible effect that vanishes in the high-dimensional regime. Furthermore, our empirical estimates (Figure 1) suggest that the surrogate expressions are accurate not only in the asymptotic limit, but even for moderately large dimensions. Based on a detailed empirical analysis described in Section 5, we conjecture that the convergence described in Theorem 3 has the rate of $O(1/d)$.

2 Related work

There is a large body of related work, which for simplicity we cluster into three groups.

Double descent. The double descent phenomenon has been observed empirically in a number of learning models, including neural networks [BHMM19, GJS⁺19], kernel methods [BMM18, BRT19], nearest neighbor models [BHM18], and decision trees [BHMM19]. The theoretical analysis of double descent, and more broadly the generalization properties of interpolating estimators, have primarily focused on various forms of linear regression [BLT19, LR19, HMRT19, MVSS19]. Note that while we analyze the classical mean squared error, many works focus on the squared prediction error. Also, unlike in our work, some of the literature on double descent deals with linear regression in the so-called *misspecified* setting, where the set of observed features does not match the feature space in which the response model is linear [BHX19, HMRT19, Mit19, MM19b], e.g., when the learner observes a random subset of d features from a larger population.

The most directly comparable to our setting is the recent work of [HMRT19]. They study how varying the feature dimension affects the (asymptotic) generalization error for linear regression, however their analysis is limited to certain special settings such as an isotropic data distribution. As an additional point of comparison, in Figure 2 we plot the MSE expressions of Theorem 1 when varying the feature dimension d (the setup is the same as in Figure 1). Our plots follow the trends outlined by [HMRT19] for the isotropic case (see their Figure 2), but the spectral decay of the covariance (captured by our new MSE expressions) has a significant effect on the descent curve. This leads to generalization in the under-determined regime even when the signal-to-noise ratio (SNR = $\|\mathbf{w}^*\|^2/\sigma^2$) is 1, unlike suggested by [HMRT19].

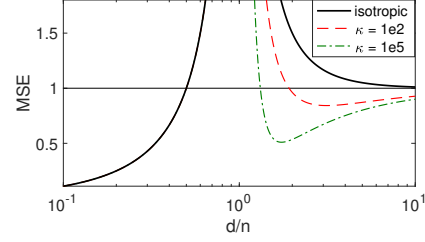


Figure 2: Surrogate MSE as a function of d/n , with n fixed to 100 and varying d , for signal-to-noise ratio SNR = 1.

RandNLA and DPPs. Randomized Numerical Linear Algebra [DM16, DM17] has traditionally focused on obtaining purely algorithmic improvements for tasks such as least squares regression, but there has been growing interest in understanding the statistical properties of these randomized methods [MMY15, RM16]. Determinantal point processes [KT12] have been recently shown to combine strong worst-case regression guarantees with elegant statistical properties [DW17]. However, these results are limited to the over-determined setting [DWH18, DWH19a, DCMW19] and ridge regression [DW18, DLM19]. Our results are also related to recent work on using DPPs to analyze the expectation of the inverse [DM19] and generalized inverse [MDK19] of a subsampled matrix.

Implicit regularization. The term implicit regularization typically refers to the notion that approximate computation can implicitly lead to statistical regularization. See [MO11, PM11, GM14] and references therein for early work on the topic; and see [Mah12] for an overview. More recently, often motivated by neural networks, there has been work on implicit regularization that typically considered SGD-based optimization algorithms. See, e.g., theoretical results [NTS14, Ney17, SHN⁺18, GWB⁺17, ACHL19, KBMM19] as well as extensive empirical studies [MM18, MM19a]. The implicit regularization observed by us is different in that it is not caused by an inexact approximation algorithm (such as SGD) but rather by the selection of one out of many exact solutions (e.g., the minimum norm solution). In this context, most relevant are the asymptotic results of [KLS18] and [LJB19].

3 Surrogate random designs

In this section, we provide the definition of our surrogate random design S_μ^n , where μ is a d -variate probability measure and n is the sample size. This distribution is used in place of the standard random design μ^n consisting of n row vectors drawn independently from μ .

Preliminaries. For an $n \times n$ matrix \mathbf{A} , we use $\text{pdet}(\mathbf{A})$ to denote the pseudo-determinant of \mathbf{A} , which is the product of non-zero eigenvalues. For index subsets \mathcal{I} and \mathcal{J} , we use $\mathbf{A}_{\mathcal{I}, \mathcal{J}}$ to denote the submatrix of \mathbf{A} with rows indexed by \mathcal{I} and columns indexed by \mathcal{J} . We may write $\mathbf{A}_{\mathcal{I}, *}$ to indicate that we take a subset of rows. We let $\mathbf{X} \sim \mu^k$ denote a $k \times d$ random matrix with rows drawn i.i.d. according to μ , and the i th row is denoted as \mathbf{x}_i^\top . We also let $\Sigma_\mu = \mathbb{E}_\mu[\mathbf{x}\mathbf{x}^\top]$, where \mathbb{E}_μ refers to the expectation with respect to $\mathbf{x}^\top \sim \mu$, assuming throughout that Σ_μ is well-defined and positive definite. We use $\text{Poisson}(\gamma)_{\leq a}$ as the Poisson distribution restricted to $[0, a]$, whereas $\text{Poisson}(\gamma)_{\geq a}$ is restricted to $[a, \infty)$. We also let $\#(\mathbf{X})$ denote the number of rows of \mathbf{X} .

Definition 2 Let μ satisfy Assumption 2 and let K be a random variable over $\mathbb{Z}_{\geq 0}$. A determinantal design $\tilde{\mathbf{X}} \sim \text{Det}(\mu, K)$ is a distribution with the same domain as $\mathbf{X} \sim \mu^K$ such that for any event E measurable w.r.t. \mathbf{X} , we have

$$\Pr\{\tilde{\mathbf{X}} \in E\} = \frac{\mathbb{E}[\text{pdet}(\mathbf{X}\mathbf{X}^\top)\mathbf{1}_{\{\mathbf{X} \in E\}}]}{\mathbb{E}[\text{pdet}(\mathbf{X}\mathbf{X}^\top)]}.$$

The above definition can be interpreted as rescaling the density function of μ^K by the pseudo-determinant, and then renormalizing it. We now construct our surrogate design S_μ^n by appropriately selecting the random variable K . The obvious choice of $K = n$ does not result in simple closed form expressions for the MSE in the under-determined regime (i.e., $n < d$), which is the regime of primary interest to us. Instead, we derive our random variables K from the Poisson distribution.

213 **Definition 3** For μ satisfying Assumption 2, define surrogate design S_μ^n as $\text{Det}(\mu, K)$ where:

- 214 1. if $n < d$, then $K \sim \text{Poisson}(\gamma_n)_{\leq d}$ with γ_n as the solution of $n = \text{tr}(\Sigma_\mu(\Sigma_\mu + \frac{1}{\gamma_n}\mathbf{I})^{-1})$,
 215 2. if $n = d$, then we simply let $K = d$,
 216 3. if $n > d$, then $K \sim \text{Poisson}(\gamma_n)_{\geq d}$ with $\gamma_n = n - d$.

217 Note that the under-determined case, i.e., $n < d$, is restricted to $K \leq d$ so that, under Assumption 2,
 218 $\text{pdet}(\mathbf{X}\mathbf{X}^\top) = \det(\mathbf{X}\mathbf{X}^\top)$ with probability 1. On the other hand in the over-determined case, i.e.,
 219 $n > d$, we have $K \geq d$ so that $\text{pdet}(\mathbf{X}\mathbf{X}^\top) = \det(\mathbf{X}^\top\mathbf{X})$. In the special case of $n = d = K$ both
 220 of these equations are satisfied: $\text{pdet}(\mathbf{X}\mathbf{X}^\top) = \det(\mathbf{X}^\top\mathbf{X}) = \det(\mathbf{X}\mathbf{X}^\top) = \det(\mathbf{X})^2$.

221 The first non-trivial property of the surrogate design S_μ^n is that the expected sample size is in fact
 222 always equal to n , which we prove in Appendix A.

223 **Lemma 1** Let $\bar{\mathbf{X}} \sim S_\mu^n$ for any $n > 0$. Then, we have $\mathbb{E}[\#(\bar{\mathbf{X}})] = n$.

224 Our general template for computing expectations under a surrogate design $\bar{\mathbf{X}} \sim S_\mu^n$ is to use the
 225 following expressions based on the i.i.d. random design $\mathbf{X} \sim \mu^K$:

$$\mathbb{E}[F(\bar{\mathbf{X}})] = \begin{cases} \frac{\mathbb{E}[\det(\mathbf{X}\mathbf{X}^\top)F(\mathbf{X})]}{\mathbb{E}[\det(\mathbf{X}\mathbf{X}^\top)]} & K \sim \text{Poisson}(\gamma_n) \quad \text{for } n < d, \\ \frac{\mathbb{E}[\det(\mathbf{X})^2 F(\mathbf{X})]}{\mathbb{E}[\det(\mathbf{X})^2]} & K = d \quad \text{for } n = d, \\ \frac{\mathbb{E}[\det(\mathbf{X}^\top\mathbf{X})F(\mathbf{X})]}{\mathbb{E}[\det(\mathbf{X}^\top\mathbf{X})]} & K \sim \text{Poisson}(\gamma_n) \quad \text{for } n > d. \end{cases} \quad (1)$$

226 These formulas follow from Definitions 2 and 3 because the determinants $\det(\mathbf{X}\mathbf{X}^\top)$ and $\det(\mathbf{X}^\top\mathbf{X})$
 227 are non-zero precisely in the regimes $n \leq d$ and $n \geq d$, respectively, which is why we can drop the
 228 restrictions on the range of the Poisson distribution. We compute the normalization constants by
 229 introducing the concept of determinant preserving random matrices, discussed in Section 4.

230 **Proof sketch of Theorem 1** We focus here on the under-determined regime (i.e., $n < d$), high-
 231 lighting the key new expectation formulas we develop to derive the MSE expressions for surrogate
 232 designs. A standard decomposition of the MSE yields:

$$\text{MSE}[\bar{\mathbf{X}}^\dagger \bar{\mathbf{y}}] = \mathbb{E}[\|\bar{\mathbf{X}}^\dagger(\bar{\mathbf{X}}\mathbf{w}^* + \boldsymbol{\xi}) - \mathbf{w}^*\|^2] = \sigma^2 \mathbb{E}[\text{tr}((\bar{\mathbf{X}}^\top \bar{\mathbf{X}})^\dagger)] + \mathbf{w}^{*\top} \mathbb{E}[\mathbf{I} - \bar{\mathbf{X}}^\dagger \bar{\mathbf{X}}] \mathbf{w}^*. \quad (2)$$

233 Thus, our task is to find closed form expressions for the two expectations above. The latter, which is
 234 the expected projection onto the complement of the row-span of $\bar{\mathbf{X}}$, is proven in Appendix D.

235 **Lemma 2** If $\bar{\mathbf{X}} \sim S_\mu^n$ and $n < d$, then we have: $\mathbb{E}[\mathbf{I} - \bar{\mathbf{X}}^\dagger \bar{\mathbf{X}}] = (\gamma_n \Sigma_\mu + \mathbf{I})^{-1}$.

236 No such expectation formula is known for i.i.d. designs, except when μ is an isotropic Gaussian.
 237 In Appendix D, we also prove a generalization of Lemma 2 which is then used to establish our
 238 implicit regularization result (Theorem 2). We next give an expectation formula for the trace of the
 239 Moore-Penrose inverse of the covariance matrix for a surrogate design (proof in Appendix C).

240 **Lemma 3** If $\bar{\mathbf{X}} \sim S_\mu^n$ and $n < d$, then: $\mathbb{E}[\text{tr}((\bar{\mathbf{X}}^\top \bar{\mathbf{X}})^\dagger)] = \gamma_n (1 - \det((\frac{1}{\gamma_n} \mathbf{I} + \Sigma_\mu)^{-1} \Sigma_\mu))$.

241 Note the implicit regularization term which appears in both formulas, given by $\lambda_n = \frac{1}{\gamma_n}$. Since $n =$
 242 $\text{tr}(\Sigma_\mu(\Sigma_\mu + \lambda_n \mathbf{I})^{-1}) = d - \lambda_n \text{tr}((\Sigma_\mu + \lambda_n \mathbf{I})^{-1})$, it follows that $\lambda_n = (d - n)/\text{tr}((\Sigma_\mu + \lambda_n \mathbf{I})^{-1})$.
 243 Combining this with Lemmas 2 and 3, we recover the surrogate MSE expression in Theorem 1.

244 4 Determinant preserving random matrices

245 In this section, we introduce the key tool for computing expectation formulas of matrix determinants.
 246 It is used in our analysis of the surrogate design, and it should be of independent interest.

247 The key question motivating the following definition is: *When does taking expectation commute with*
 248 *computing a determinant for a square random matrix?*

249 **Definition 4** A random $d \times d$ matrix \mathbf{A} is called determinant preserving (d.p.), if

$$\mathbb{E}[\det(\mathbf{A}_{\mathcal{I}, \mathcal{J}})] = \det(\mathbb{E}[\mathbf{A}_{\mathcal{I}, \mathcal{J}}]) \quad \text{for all } \mathcal{I}, \mathcal{J} \subseteq [d] \text{ s.t. } |\mathcal{I}| = |\mathcal{J}|.$$

250 We next give a few simple examples to provide some intuition. First, note that every 1×1 random
 251 matrix is determinant preserving simply because taking a determinant is an identity transformation in
 252 one dimension. Similarly, every fixed matrix is determinant preserving because in this case taking the
 253 expectation is an identity transformation. In all other cases, however, Definition 4 has to be verified
 254 more carefully. Further examples (positive and negative) follow.

255 **Example 1** If \mathbf{A} has i.i.d. Gaussian entries $a_{ij} \sim \mathcal{N}(0, 1)$, then \mathbf{A} is d.p. because $\mathbb{E}[\det(\mathbf{A})] = 0$.

256 In fact, it can be shown that all random matrices with independent entries are determinant preserving.
 257 However, this is not a necessary condition.

258 **Example 2** Let $\mathbf{A} = s\mathbf{Z}$, where \mathbf{Z} is fixed with $\text{rank}(\mathbf{Z}) = r$, and s is a scalar random variable.
 259 Then for $|\mathcal{I}| = |\mathcal{J}| = r$ we have

$$\mathbb{E}[\det(s\mathbf{Z}_{\mathcal{I},\mathcal{J}})] = \mathbb{E}[s^r] \det(\mathbf{Z}_{\mathcal{I},\mathcal{J}}) = \det\left(\left(\mathbb{E}[s^r]\right)^{\frac{1}{r}} \mathbf{Z}_{\mathcal{I},\mathcal{J}}\right),$$

260 so if $r = 1$ then \mathbf{A} is determinant preserving, whereas if $r > 1$ and $\text{Var}[s] > 0$ then it is not.

261 To construct more complex examples, we show that determinant preserving random matrices are
 262 closed under addition and multiplication. The proof of this result is an extension of an existing
 263 argument, given by [DM19] in the proof of Lemma 7, for computing the expected determinant of the
 264 sum of rank-1 random matrices (proof in Appendix B).

265 **Lemma 4 (Closure properties)** If \mathbf{A} and \mathbf{B} are independent and determinant preserving, then:

- 266 1. $\mathbf{A} + \mathbf{B}$ is determinant preserving,
- 267 2. \mathbf{AB} is determinant preserving.

268 Next, we introduce another important class of d.p. matrices: a sum of i.i.d. rank-1 random matrices
 269 with the number of i.i.d. samples being a Poisson random variable. Our use of the Poisson distribution
 270 is crucial for the below result to hold. It is an extension of an expectation formula given by [Der19]
 271 for sampling from discrete distributions (proof in Appendix B).

272 **Lemma 5** If K is a Poisson random variable and \mathbf{A}, \mathbf{B} are random $K \times d$ matrices whose rows are
 273 sampled as an i.i.d. sequence of joint pairs of random vectors, then $\mathbf{A}^\top \mathbf{B}$ is d.p., and so:

$$\mathbb{E}[\det(\mathbf{A}^\top \mathbf{B})] = \det(\mathbb{E}[\mathbf{A}^\top \mathbf{B}]).$$

274 Finally, we show the expectation formula needed for obtaining the normalization constant of the under-
 275 determined surrogate design, given in (1). The below result is more general than the normalization
 276 constant requires, because it allows the matrices \mathbf{A} and \mathbf{B} to be different (the constant is obtained by
 277 setting $\mathbf{A} = \mathbf{B} = \mathbf{X} \sim \mu^K$). In fact, we use this more general statement to show Theorems 1 and 2.
 278 The proof uses Lemmas 4 and 5 (see Appendix B).

279 **Lemma 6** If K is a Poisson random variable and \mathbf{A}, \mathbf{B} are random $K \times d$ matrices whose rows are
 280 sampled as an i.i.d. sequence of joint pairs of random vectors, then

$$\mathbb{E}[\det(\mathbf{AB}^\top)] = e^{-\mathbb{E}[K]} \det(\mathbf{I} + \mathbb{E}[\mathbf{B}^\top \mathbf{A}]).$$

281 5 Empirical evaluation of asymptotic consistency

282 In this section, we empirically quantify the convergence rates for the asymptotic result of Theorem 3.
 283 We focus on the under-determined regime (i.e., $n < d$) and separate the evaluation into the bias and
 284 variance terms, following the MSE decomposition given in (2). Consider $\mathbf{X} = \mathbf{Z}\Sigma^{1/2}$, where the
 285 entries of \mathbf{Z} are i.i.d. standard Gaussian, and define:

- 286 1. Variance discrepancy: $\left| \frac{\mathbb{E}[\text{tr}((\mathbf{X}^\top \mathbf{X})^\dagger)]}{\mathcal{V}(\Sigma, n)} - 1 \right|$ where $\mathcal{V}(\Sigma, n) = \frac{1-\alpha_n}{\lambda_n}$.
- 287 2. Bias discrepancy: $\sup_{\mathbf{w} \in \mathbb{R}^d \setminus \{0\}} \left| \frac{\mathbf{w}^\top \mathbb{E}[\mathbf{I} - \mathbf{X}^\dagger \mathbf{X}] \mathbf{w}}{\mathbf{w}^\top \mathcal{B}(\Sigma, n) \mathbf{w}} - 1 \right|$ where $\mathcal{B}(\Sigma, n) = \lambda_n(\Sigma + \lambda_n \mathbf{I})^{-1}$.

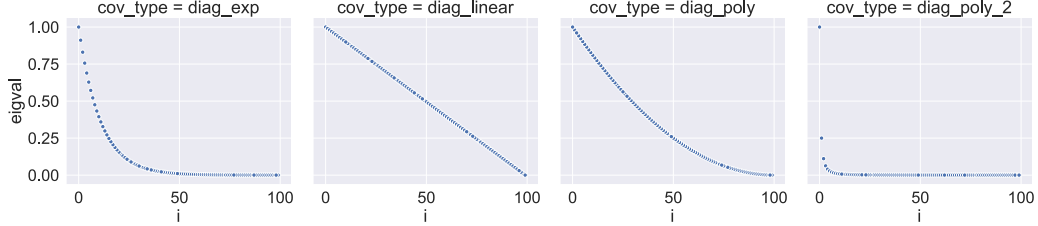


Figure 3: Scree-plots of Σ for the eigenvalue decays examined in our empirical valuations.

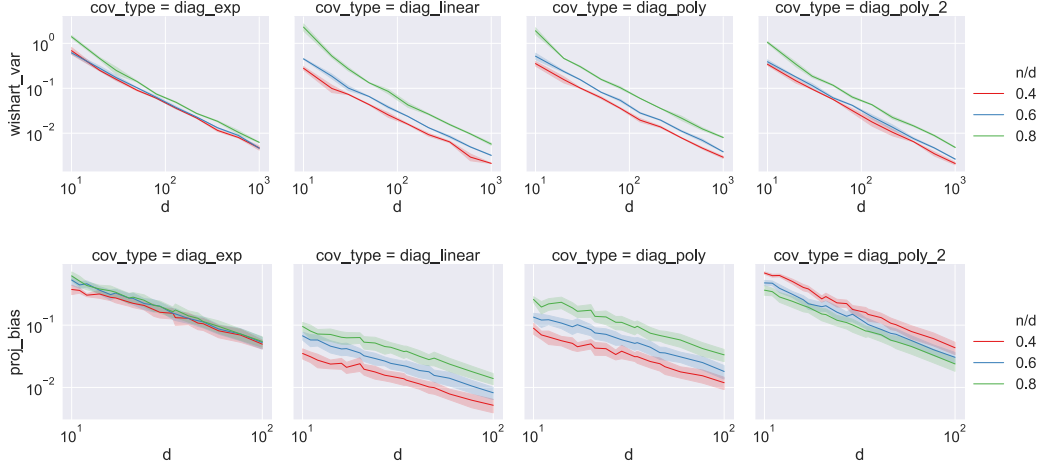


Figure 4: Empirical verification of the asymptotic consistency of surrogate MSE. We show the discrepancies for the variance (top) and bias (bottom), with bootstrapped 95% confidence intervals, as d increases and n/d is fixed. We observe $O(1/d)$ decay (linear with slope -1 on a log-log plot).

Recall that $\lambda_n = \frac{d-n}{\text{tr}((\Sigma + \lambda_n \mathbf{I})^{-1})}$, so our surrogate MSE can be written as $\mathcal{M} = \sigma^2 \mathcal{V}(\Sigma, n) + \mathbf{w}^{*\top} \mathcal{B}(\Sigma, n) \mathbf{w}^*$, and when both discrepancies are bounded by ϵ , then $(1 - 2\epsilon)\mathcal{M} \leq \text{MSE}[\mathbf{X}^\dagger \mathbf{y}] \leq (1 + 2\epsilon)\mathcal{M}$. In our experiments, we consider four standard eigenvalue decay profiles for Σ , including polynomial and exponential decay (see Figure 3 and Appendix F.1).

Figure 4 (top) plots the variance discrepancy (with $\mathbb{E}[\text{tr}((\mathbf{X}^\top \mathbf{X})^\dagger)]$ estimated via Monte Carlo sampling and bootstrapped confidence intervals) as d increases from 10 to 1000, across a range of aspect ratios n/d . In all cases, we observe that the discrepancy decays to zero at a rate of $O(1/d)$. Figure 4 (bottom) plots the bias discrepancy, with the same rate of decay observed throughout. Note that the range of d is smaller than in Figure 4 (top) because the large number of Monte Carlo samples (up to two million) required for this experiment made the computations much more expensive (more details in Appendix F). Based on the above empirical results, we conclude with a conjecture.

Conjecture 1 When μ is a centered multivariate Gaussian and its covariance has a constant condition number; then, for n/d fixed, the surrogate MSE satisfies: $\left| \frac{\text{MSE}[\mathbf{X}^\dagger \mathbf{y}]}{\mathcal{M}} - 1 \right| = O(1/d)$.

6 Conclusions

We derived exact non-asymptotic expressions for the MSE of the Moore-Penrose estimator in the linear regression task, reproducing the double descent phenomenon as the sample size crosses between the under- and over-determined regime. To achieve this, we modified the standard i.i.d. random design distribution using a determinantal point process to obtain a surrogate design which admits exact MSE expressions, while capturing the key properties of the i.i.d. design. We also provided a result that relates the expected value of the Moore-Penrose estimator of a training sample in the under-determined regime (i.e., the minimum norm solution) to the ridge-regularized least squares solution for the population distribution, thereby providing an interpretation for the implicit regularization resulting from over-parameterization.

Broader Impact

While the double descent phenomenon has been empirically observed in a variety of applications, mathematical descriptions of it are oftentimes complex and inaccessible to non-experts. In contrast, our surrogate design and the accompanying closed-form expressions provide an easily computable rule of thumb for estimating the generalization error. One important application is the high-dimensional (i.e. underdetermined, $n < d$) regime experienced by modern machine learning systems where the number of parameters vastly exceeds the quantity of available data. Our research can be applied here to provide a theoretical understanding of the surprising phenomenon where more data leads to worse generalization performance.

Better theoretical understanding of generalization error in the small data regime has important societal impact. Through theoretically modeling a system’s performance, we can build safer systems by better understanding how badly an estimator fails and accounting for these failure modes in the system’s design. Furthermore, the improved understanding of minimum norm solutions performing worse with more data offers an appealing trade-off where certain systems can both improve their performance and respect the privacy of its users by collecting less data.

References

- [ACHL19] Sanjeev Arora, Nadav Cohen, Wei Hu, and Yuping Luo. Implicit regularization in deep matrix factorization. In H. Wallach, H. Larochelle, A. Beygelzimer, F. d Alché-Buc, E. Fox, and R. Garnett, editors, *Advances in Neural Information Processing Systems 32*, pages 7411–7422. Curran Associates, Inc., 2019.
- [AM15] Ahmed El Alaoui and Michael W. Mahoney. Fast randomized kernel ridge regression with statistical guarantees. In *Proceedings of the 28th International Conference on Neural Information Processing Systems*, pages 775–783, Montreal, Canada, December 2015.
- [Ber11] Dennis S. Bernstein. *Matrix Mathematics: Theory, Facts, and Formulas*. Princeton University Press, second edition, 2011.
- [BHM18] Mikhail Belkin, Daniel J Hsu, and Partha Mitra. Overfitting or perfect fitting? Risk bounds for classification and regression rules that interpolate. In S. Bengio, H. Wallach, H. Larochelle, K. Grauman, N. Cesa-Bianchi, and R. Garnett, editors, *Advances in Neural Information Processing Systems 31*, pages 2300–2311. Curran Associates, Inc., 2018.
- [BHMM19] M. Belkin, D. Hsu, S. Ma, and S. Mandal. Reconciling modern machine-learning practice and the classical bias–variance trade-off. *Proc. Natl. Acad. Sci. USA*, 116:15849–15854, 2019.
- [BHX19] Mikhail Belkin, Daniel Hsu, and Ji Xu. Two models of double descent for weak features. *arXiv preprint arXiv:1903.07571*, 2019.
- [BLLT19] P. L. Bartlett, P. M. Long, G. Lugosi, and A. Tsigler. Benign overfitting in linear regression. Technical Report Preprint: arXiv:1906.11300, 2019.
- [BMM18] M. Belkin, S. Ma, and S. Mandal. To understand deep learning we need to understand kernel learning. In *Proceedings of the 35th International Conference on Machine Learning*, volume 80 of *Proceedings of Machine Learning Research*, Stockholm, Sweden, 2018. PMLR.
- [BRT19] M. Belkin, A. Rakhlin, and A. B. Tsybakov. Does data interpolation contradict statistical optimality? In *Proceedings of the 22nd International Conference on Artificial Intelligence and Statistics*, volume 89 of *Proceedings of Machine Learning Research*, Naha, Okinawa, Japan, 2019. PMLR.
- [BS⁺98] Zhi-Dong Bai, Jack W Silverstein, et al. No eigenvalues outside the support of the limiting spectral distribution of large-dimensional sample covariance matrices. *The Annals of Probability*, 26(1):316–345, 1998.

360 [BY⁺93] ZD Bai, YQ Yin, et al. Limit of the smallest eigenvalue of a large dimensional sample
361 covariance matrix. *The Annals of Probability*, 21(3):1275–1294, 1993.

362 [CF11] R. Dennis Cook and Liliana Forzani. On the mean and variance of the generalized
363 inverse of a singular wishart matrix. *Electron. J. Statist.*, 5:146–158, 2011.

364 [Chi90] Yasuko Chikuse. The matrix angular central gaussian distribution. *Journal of Multi-*
365 *variate Analysis*, 33(2):265–274, 1990.

366 [Chi91] Yasuko Chikuse. High dimensional limit theorems and matrix decompositions on the
367 stiefel manifold. *Journal of Multivariate Analysis*, 36(2):145 – 162, 1991.

368 [Chi98] Yasuko Chikuse. Density estimation on the stiefel manifold. *Journal of Multivariate*
369 *Analysis*, 66(2):188 – 206, 1998.

370 [DCMW19] Michał Dereziński, Kenneth L. Clarkson, Michael W. Mahoney, and Manfred K. War-
371 muth. Minimax experimental design: Bridging the gap between statistical and worst-
372 case approaches to least squares regression. In Alina Beygelzimer and Daniel Hsu,
373 editors, *Proceedings of the Thirty-Second Conference on Learning Theory*, volume 99 of
374 *Proceedings of Machine Learning Research*, pages 1050–1069, Phoenix, USA, 25–28
375 Jun 2019.

376 [Der19] Michał Dereziński. Fast determinantal point processes via distortion-free intermediate
377 sampling. In Alina Beygelzimer and Daniel Hsu, editors, *Proceedings of the Thirty-*
378 *Second Conference on Learning Theory*, volume 99 of *Proceedings of Machine Learning*
379 *Research*, pages 1029–1049, Phoenix, USA, 25–28 Jun 2019.

380 [DLM19] Michał Dereziński, Feynman Liang, and Michael W. Mahoney. Bayesian experi-
381 mental design using regularized determinantal point processes. *arXiv e-prints*, page
382 arXiv:1906.04133, Jun 2019.

383 [DM16] Petros Drineas and Michael W. Mahoney. RandNLA: Randomized numerical linear
384 algebra. *Communications of the ACM*, 59:80–90, 2016.

385 [DM17] Petros Drineas and Michael W. Mahoney. Lectures on randomized numerical linear
386 algebra. Technical report, 2017. Preprint: arXiv:1712.08880; To appear in: *Lectures of*
387 *the 2016 PCMI Summer School on Mathematics of Data*.

388 [DM19] Michał Dereziński and Michael W Mahoney. Distributed estimation of the inverse
389 hessian by determinantal averaging. In H. Wallach, H. Larochelle, A. Beygelzimer,
390 F. d Alché-Buc, E. Fox, and R. Garnett, editors, *Advances in Neural Information*
391 *Processing Systems 32*, pages 11401–11411. Curran Associates, Inc., 2019.

392 [DW17] Michał Dereziński and Manfred K. Warmuth. Unbiased estimates for linear regression
393 via volume sampling. In *Advances in Neural Information Processing Systems 30*, pages
394 3087–3096, Long Beach, CA, USA, 2017.

395 [DW18] Michał Dereziński and Manfred K. Warmuth. Subsampling for ridge regression via
396 regularized volume sampling. In Amos Storkey and Fernando Perez-Cruz, editors,
397 *Proceedings of the Twenty-First International Conference on Artificial Intelligence and*
398 *Statistics*, pages 716–725, Playa Blanca, Lanzarote, Canary Islands, April 2018.

399 [DWH18] Michał Dereziński, Manfred K. Warmuth, and Daniel Hsu. Leveraged volume sampling
400 for linear regression. In S. Bengio, H. Wallach, H. Larochelle, K. Grauman, N. Cesa-
401 Bianchi, and R. Garnett, editors, *Advances in Neural Information Processing Systems*
402 *31*, pages 2510–2519. Curran Associates, Inc., 2018.

403 [DWH19a] Michał Dereziński, Manfred K. Warmuth, and Daniel Hsu. Correcting the bias in
404 least squares regression with volume-rescaled sampling. In Kamalika Chaudhuri and
405 Masashi Sugiyama, editors, *Proceedings of the 22nd International Conference on*
406 *Artificial Intelligence and Statistics*, volume 89 of *Proceedings of Machine Learning*
407 *Research*, pages 944–953. PMLR, 16–18 Apr 2019.

408 [DWH19b] Michał Dereziński, Manfred K. Warmuth, and Daniel Hsu. Unbiased estimators for
409 random design regression. *arXiv e-prints*, page arXiv:1907.03411, Jul 2019.

410 [FHT01] Jerome Friedman, Trevor Hastie, and Robert Tibshirani. *The elements of statistical*
411 *learning*, volume 1. Springer series in statistics New York, 2001.

412 [GJS⁺19] M. Geiger, A. Jacot, S. Spigler, F. Gabriel, L. Sagun, S. d’Ascoli, G. Biroli, C. Hongler,
413 and M. Wyart. Scaling description of generalization with number of parameters in deep
414 learning. Technical Report Preprint: arXiv:1901.01608, 2019.

415 [GM14] D. F. Gleich and M. W. Mahoney. Anti-differentiating approximation algorithms: A
416 case study with min-cuts, spectral, and flow. In *Proceedings of the 31st International*
417 *Conference on Machine Learning*, pages 1018–1025, 2014.

418 [GWB⁺17] Suriya Gunasekar, Blake E Woodworth, Srinadh Bhojanapalli, Behnam Neyshabur, and
419 Nati Srebro. Implicit regularization in matrix factorization. In I. Guyon, U. V. Luxburg,
420 S. Bengio, H. Wallach, R. Fergus, S. Vishwanathan, and R. Garnett, editors, *Advances*
421 *in Neural Information Processing Systems 30*, pages 6151–6159. Curran Associates,
422 Inc., 2017.

423 [HLNV13] Walid Hachem, Philippe Loubaton, Jamal Najim, and Pascal Vallet. On bilinear forms
424 based on the resolvent of large random matrices. *Annales de l’IHP Probabilités et*
425 *statistiques*, 49(1):36–63, 2013.

426 [HMRT19] T. Hastie, A. Montanari, S. Rosset, and R. J. Tibshirani. Surprises in high-dimensional
427 ridgeless least squares interpolation. Technical Report Preprint: arXiv:1903.08560,
428 2019.

429 [KBMM19] M. Kubo, R. Banno, H. Manabe, and M. Minoji. Implicit regularization in over-
430 parameterized neural networks. Technical Report Preprint: arXiv:1903.01997, 2019.

431 [KLS18] D. Kobak, J. Lomond, and B. Sanchez. Optimal ridge penalty for real-world high-
432 dimensional data can be zero or negative due to the implicit ridge regularization.
433 Technical report, 2018. Preprint: arXiv:1805.10939.

434 [KT12] Alex Kulesza and Ben Taskar. *Determinantal Point Processes for Machine Learning*.
435 Now Publishers Inc., Hanover, MA, USA, 2012.

436 [LEM19] Miles E Lopes, N Benjamin Erichson, and Michael W Mahoney. Bootstrapping
437 the operator norm in high dimensions: Error estimation for covariance matrices and
438 sketching. *arXiv preprint arXiv:1909.06120*, 2019.

439 [LJB19] D. LeJeune, H. Javadi, and R. G. Baraniuk. The implicit regularization of ordinary least
440 squares ensembles. Technical report, 2019. Preprint: arXiv:1910.04743.

441 [LP11] Olivier Ledoit and Sandrine Pécché. Eigenvectors of some large sample covariance
442 matrix ensembles. *Probability Theory and Related Fields*, 151(1-2):233–264, 2011.

443 [LR19] T. Liang and A. Rakhlin. Just interpolate: Kernel “ridgeless” regression can generalize.
444 *The Annals of Statistics*, to appear, 2019.

445 [Mah12] M. W. Mahoney. Approximate computation and implicit regularization for very large-
446 scale data analysis. In *Proceedings of the 31st ACM Symposium on Principles of*
447 *Database Systems*, pages 143–154, 2012.

448 [MDK19] M. Mutný, M. Dereziński, and A. Krause. Convergence analysis of the random-
449 ized Newton method with determinantal sampling. Technical report, 2019. Preprint:
450 arXiv:1910.11561.

451 [Mit19] P. P. Mitra. Understanding overfitting peaks in generalization error: Analyti-
452 cal risk curves for l2 and l1 penalized interpolation. Technical Report Preprint:
453 arXiv:1906.03667, 2019.

454 [MM18] C. H. Martin and M. W. Mahoney. Implicit self-regularization in deep neural networks:
455 Evidence from random matrix theory and implications for learning. Technical Report
456 Preprint: arXiv:1810.01075, 2018.

457 [MM19a] C. H. Martin and M. W. Mahoney. Traditional and heavy-tailed self regularization
458 in neural network models. In *Proceedings of the 36th International Conference on*
459 *Machine Learning*, pages 4284–4293, 2019.

460 [MM19b] S. Mei and A. Montanari. The generalization error of random features regres-
461 sion: Precise asymptotics and double descent curve. Technical Report Preprint:
462 arXiv:1908.05355, 2019.

463 [MMY15] P. Ma, M. W. Mahoney, and B. Yu. A statistical perspective on algorithmic leveraging.
464 *Journal of Machine Learning Research*, 16:861–911, 2015.

465 [MO11] M. W. Mahoney and L. Orecchia. Implementing regularization implicitly via approxi-
466 mate eigenvector computation. In *Proceedings of the 28th International Conference on*
467 *Machine Learning*, pages 121–128, 2011.

468 [MVSS19] V. Muthukumar, K. Vodrahalli, V. Subramanian, and A. Sahai. Harmless interpolation
469 of noisy data in regression. Technical Report Preprint: arXiv:1903.09139, 2019.

470 [Ney17] B. Neyshabur. Implicit regularization in deep learning. Technical report, 2017. Preprint:
471 arXiv:1709.01953.

472 [NTS14] B. Neyshabur, R. Tomioka, and N. Srebro. In search of the real inductive bias: on the role
473 of implicit regularization in deep learning. Technical Report Preprint: arXiv:1412.6614,
474 2014.

475 [PM11] P. O. Perry and M. W. Mahoney. Regularized Laplacian estimation and fast eigenvector
476 approximation. In *Annual Advances in Neural Information Processing Systems 24: Proceedings of the 2011 Conference*, 2011.

477 [RM16] G. Raskutti and M. W. Mahoney. A statistical perspective on randomized sketching for
478 ordinary least-squares. *Journal of Machine Learning Research*, 17(214):1–31, 2016.

480 [SB95] Jack W Silverstein and ZD Bai. On the empirical distribution of eigenvalues of a class
481 of large dimensional random matrices. *Journal of Multivariate analysis*, 54(2):175–192,
482 1995.

483 [SHN⁺18] Daniel Soudry, Elad Hoffer, Mor Shpigel Nacson, Suriya Gunasekar, and Nathan
484 Srebro. The implicit bias of gradient descent on separable data. *The Journal of Machine*
485 *Learning Research*, 19(1):2822–2878, 2018.

486 [Sri03] M.S. Srivastava. Singular wishart and multivariate beta distributions. *Ann. Statist.*,
487 31(5):1537–1560, 10 2003.

488 [vdV65] H. Robert van der Vaart. A note on Wilks’ internal scatter. *Ann. Math. Statist.*,
489 36(4):1308–1312, 08 1965.